Membrane and Water Treatment, *Vol. 12, No. 3 (2021) 107-114*
DOI: https://doi.org/10.12989/mwt.2021.12.3.107

Multiscale calculation results of the flow behavior in micro/nano porous filtration membrane with the adsorbed layer-fluid interfacial slippage

Jian Li[1,2] and Yongbin Zhang*[1]

[1]*College of Mechanical Engineering, Changzhou University, Changzhou, Jiangsu Province, China*
[2]*Changzhou High Technology Research Key Laboratory of Mould Advanced Manufacturing, Changzhou, Jiangsu Province, China*

(Received January 18, 2021, Revised April 14, 2021, Accepted April 16, 2021)

Abstract. The paper presents the multiscale calculation results for the multiscale flow in micro/nano porous filtration membranes where the adsorbed layer effect is involved, by considering the adsorbed layer-fluid interfacial slippage. The analysis consists of the molecular scale analysis for the adsorbed layer flow and the continuum analysis for the intermediate fluid flow. The calculation results are respectively compared with the classical flow theory calculations and those based on the solid layer assumption. The adsorbed layer flow rate is also compared with the flow rate of the intermediate continuum fluid. It is shown that for a strong fluid-pore wall interaction or for a large adsorbed layer-fluid interfacial slippage the adsorbed layer can be treated as a solid layer; otherwise it should be treated as a flowing layer. The large interfacial slippage results in the flow rate through the pore far greater than the classical Hagen-Poiseuille equation calculation; it largely propels the flow of the intermediate continuum fluid and makes the adsorbed layer flow negligible particularly for the medium and strong fluid-pore wall interactions. The increasing fluid-pore wall interaction strength significantly reduces the flow rate through the pore.

Keywords: adsorbed layer; flow; interfacial slippage; micro/nano pore; multiscale

1. Introduction

Nanoporous filtration membranes have been in fast development because of their important applications in super purification, hemofiltration, drug delivery, biosensors and DNA analysis etc. (Fissel *et al*. 2009, Jackson and Hillmyer 2010, Jung *et al*. 2019, Rashidi *et al*. 2020, Sofos *et al*. 2019, 2020, Surwade *et al*. 2015, Yang *et al*. 2006). The studies on these membranes were mainly experimental (Baker and Bird 2008, Jung *et al*. 2019, Li *et al*. 2004, Rashidi *et al*. 2020, Tiraferri *et al*. 2011, Yip *et al*. 2010). It has been found by experiments that the water transport through carbon nanotubes is much faster than the classical hydrodynamic flow theory prediction (Calabrò 2017, Majumder *et al*. 2005, Mattia *et al*. 2014, Whitby and Quirke 2007). It was explained by using the wall slippage, the depletion layer near the wall or both of them (Calabrò *et al*. 2013, Mattia and Calabro 2012). Water can also flow in hydrophilic micro/nano tubes where there may be a certain adsorption layer on the tube wall considerably influencing the water flow (Omidvar *et al*. 2015).

In some nanoporous filtration membranes, there exists the regime of the multiscale flow where the radius of the filtration pore is comparable to the thickness of the physically adsorbed layer on the pore wall; in the central region of the pore occurs the continuum fluid flow. Theoretical studies should solve this multiscale flow.

*Corresponding author, Professor
E-mail: engmech1@sina.com

Experiments confirmed the existence of the physical adsorbed layer on a solid surface long time ago (Brown *et al*. 1975, Debye and Cleland 1959, Everett and Findenegg 1969, Findenegg 1971). The adsorbed layer can be a mono fluid molecule layer for long-chain fluid molecules or consists of several fluid molecule layers for short-chain fluid molecules or simple fluids. The mono adsorbed layer can be taken as a solid layer (Grosse-Rhode and Findenegg 1978), while the multiple adsorbed fluid molecule layers should be treated by considering the momentum transfer between them (Zhang 2006).

Not only the orientation but also the density and viscosity evolution occur within the adsorbed layer (Abraham 1978, Derjaguin 1983, Kern *et al*. 1977, Somers and Davis 1992). These physical phenomena depend on the fluid-solid interaction, the solid structure and the temperature. A simple way is just treating the adsorbed layer and the intermediate continuum fluid respectively with different viscosities (Chan and Horn 1985, Chauveteau *et al*. 1984), however, it was also realized that the microscopic molecular-scale flow model should be required for the adsorbed layer flow.

Chan and Horn (1985) experimentally detected the adsorbed layer effect in a concentrated contact which resulted in the anomalous flow behavior between two solid surfaces when the surface separation was below 50nm. From their experiment, it should still not be drawn that the flow has entered into the non-continuum regime for the surface separation below 50 nm. There may be the multiscale flow in their experiment consisting of both the adsorbed layer flow and the intermediate continuum fluid flow. Zhang (2019) showed that the adsorbed layer with the

ISSN: 2005-8624 (Print), 2092-7037 (Online)

thickness 1nm can have a significant influence on the flow in a micro/nano slit pore when the surface separation is 50 nm.

It is necessary to develop the corresponding multiscale analysis for the multiscale flow in a micro surface separation where the adsorbed layer effect is involved. Molecular dynamics simulation was ever used to model this multiscale flow (Atkas and Aluru 2002, Liu *et al*. 2007, Nie *et al*. 2004, Sun *et al*. 2010, Yen *et al*. 2007), however it is insufficient for modeling an engineering multiscale flow because of the over cost of both the computational time and the computer storage. The flow factor approach model for nanoscale flow was used to simulate the adsorbed layer flow, and it is an equivalent continuum flow model capturing the layer orientation and rheology evolution. Based on this model, the multiscale analysis has been developed respectively for the flows in micro/nano slit and cylindrical pores (Zhang 2020a, b), the closed-form explicit flow equations have been derived respectively for the adsorbed layer flow and the intermediate continuum fluid flow (Zhang 2020a, b).

Based on the former research (Zhang 2020b) which derived the governing equations respectively for the adsorbed layer flow and the intermediate continuum fluid flow in a micro/nano cylindrical tube considering the adsorbed layer-fluid interfacial slippage, the present paper outlines the important parameters which show the adsorbed layer effect and gives the typical calculation results showing how the adsorbed layer influences the flow in micro/nano cylindrical pores in the condition of the interfacial slippage. Important conclusions have been drawn concerning the effects of both the adsorbed layer and the interfacial slippage in micro/nano cylindrical tube flows. The obtained results are of interest to the design and application of micro/nano porous filtration membranes for water purification or the separations of other liquids.

2. Studied flow

Fig. 1 shows the cross section of a micro/nano cylindrical tube where are present both the physically adsorbed boundary layer and the intermediate continuum fluid. Because of the thickness h_{bf} of the adsorbed layer on the same scale with the tube inner radius, the effect of the adsorbed layer on the tube flow should be considered. The continuum fluid flow with the covering radius R_0 can be simulated by the continuum fluid model. The fluid molecule is treated as a rigid spherical ball and within the adsorbed layer it is orientated and annularly layered as shown in Fig. 1. In a pressure driven flow, the momentum is transferred layer by layer in the proximity of the tube wall, and Fig. 1 shows the equivalent layering structure adjacent to the tube wall.

For a hydrophilic tube wall, the interfacial slippage may first occur on the adsorbed layer-fluid interface, while it is absent on the adsorbed layer-tube wall interface. This interfacial slippage should largely reduce the resistance to the continuum fluid flow and consequently significantly enhance this flow. However, the adsorbed layer flow should be significantly alleviated because of the reduced momentum transfer by the interfacial slippage. The present paper just studies this multiscale flow to show the combined effect of the adsorbed layer and the interfacial slippage.

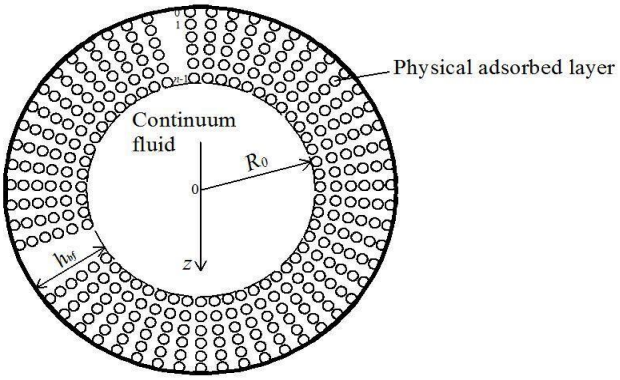

Fig. 1 The studied multiscale flow in a micro/nano cylindrical tube with the adsorbed layer-fluid interfacial slippage

3. Multiscale formulations of the flow

The detailed multiscale analysis for the tube flow in Fig. 1 has been shown by Zhang (2020b). The adsorbed layer flow is simulated by the flow factor approach model for nanoscale flow. Except on the interface, the fluid is Newtonian. The interfacial slippage is described by the limiting interfacial shear strength model, which interprets the adsorbed layer-fluid interfacial slippage as the result of the interfacial shear stress exceeding the interfacial shear strength on the adsorbed layer-fluid interface. When the magnitude of the shear stress on the adsorbed layer-fluid interface exceeds the shear strength of the adsorbed layer-fluid interface, the magnitude of the shear stress on the adsorbed layer-fluid interface will be reduced to be equal to the adsorbed layer-fluid interfacial shear strength, in this case, the shear stress boundary condition replaces the flow velocity boundary condition on the adsorbed layer-fluid interface, and by doing so there will be the flow velocity difference between the adsorbed layer and the continuum fluid on the adsorbed layer-fluid interface i.e., the interfacial slipping velocity. Furthermore, the flow is assumed as isothermal and the pressure influences on both the fluid density and viscosity are assumed as negligible.

3.1 For the adsorbed layer

When no wall slippage occurs on the tube wall but the interfacial slippage occurs on the adsorbed layer-fluid interface, the volume flow rate of the adsorbed layer through the tube is (Zhang 2020b):

$$q_{v,bf} = 2\pi R_e[\frac{h_{bf}^3}{2\eta_{bf}^{eff}}\frac{\tau_{s,b-f}}{R_0}(1+\frac{1}{2\lambda_{bf}} - \frac{q_0 - q_0^n}{q_0^{n-1} - q_0^n}\frac{\Delta_{n-2}}{h_{bf}})\frac{\varepsilon}{1+\frac{\Delta x}{D}} - \frac{F_1\tau_{s,b-f}h_{bf}^3}{12R_0\eta_{bf}^{eff}}] \quad (1)$$

where D is the fluid molecule diameter, $\tau_{s,b-f}$ is the shear

strength of the adsorbed layer-fluid interface, n is the number of the fluid molecules across the adsorbed layer thickness, R_e is an equivalent constant radius, $R_0 < R_e < R_0 + h_{bf}$, often $\frac{R_e}{R_0} = 1 + \lambda_{bf}$ and $\lambda_{bf} = \frac{h_{bf}}{2R_0}$, η_{bf}^{eff} is the effective viscosity of the adsorbed layer and formulated as $\eta_{bf}^{eff} = Dh_{bf}/[(n-1)(D+\Delta_x)(\frac{\Delta_l}{\eta_{line,l})_{avr,n-1}}$, $\eta_{line,l+1}$ and Δ_l are respectively the local viscosity and the separation between the $(l+1)^{\text{th}}$ and l^{th} fluid molecules across the layer thickness, the order number of the fluid molecules across the adsorbed layer thickness is shown in Fig. 1, $q_0 = \frac{\Delta_{l+1}}{\Delta_l}$ and q_0 (>1) is taken as the average constant, Δx is the separation between the neighboring fluid molecules in the axial direction in the adsorbed layer, ε = (2*DI* + *II*)/[*hbf*(*n*−1)($\Delta_l/\eta_{line,l}$)$_{avr,n-1}$], and $F_1 = \frac{\eta_{bf}^{eff}(12D^2\psi+6D\varphi)}{h_{bf}^3}$. Here, $i(\Delta_l/\eta_{line,l})_{avr,i} = \sum_{j=1}^{i}\frac{\Delta_{j-1}}{\eta_{line,j-1}}$, $i(l\Delta_{l-1}/\eta_{line,l-1})_{avr,i} = \sum_{j=1}^{i} j\Delta_{j-1}/\eta_{line,j-1}$, $I = \sum_{i=1}^{n-1} i(\Delta_l/\eta_{line,l})_{avr,i}$, $II = \sum_{i=0}^{n-2}[i(\Delta_l/\eta_{line,l})_{avr,i} + (i+1)(\Delta_l/\eta_{line,l})_{avr,i+1}]\Delta_i$, $\psi = \sum_{i=1}^{n-1} i(l\Delta_{l-1}/\eta_{line,l-1})_{avr,i}$, and $\varphi = \sum_{i=0}^{n-2}[i(l\Delta_{l-1}/\eta_{line,l-1})_{avr,i} + (i+1)(l\Delta_{l-1}/\eta_{line,l-1})_{avr,i+1}]\Delta_i$.

3.2 For the intermediate continuum fluid

When the interfacial slippage occurs on the adsorbed layer-fluid interface, the volume flow rate of the continuum fluid through the tube is (Zhang 2020b):

$$q_{v,hf} = \pi v_0 R_0^2 + \frac{\pi R_0^3 \tau_{s,b-f}}{4\eta} \tag{2}$$

where v_0 is the velocity of the continuum fluid at $z = -R_0$ i.e., on the adsorbed layer-fluid interface and η is the fluid bulk viscosity.

By formulating the interfacial slipping velocity as $v_s = \Delta POW/(\pi R_0 \Delta l \tau_{s,b-f})$ (Zhang 2020b), where Δl is the axial length of the tube, $\Delta POW = POW - POW_{cr}$, POW is the power loss on the tube with the axial length Δl, and POW_{cr} is the critical power loss on the tube with the axial length Δl for starting the interfacial slippage, the volume flow rate of the continuum fluid through the tube is further expressed as (Zhang 2020b):

$$q_{v,hf} = \frac{\pi R_0^3 \tau_{s,b-f}}{4\eta} + \pi R_0^2[\frac{\Delta POW}{\pi \Delta l \tau_{s,b-f} R_0} - \frac{2F_2 R_0 \tau_{s,b-f}\lambda_{bf}^2}{3\eta_{bf}^{eff}} - \frac{4R_0\tau_{s,b-f}\lambda_{bf}}{\eta_{bf}^{eff}(1+\frac{\Delta x}{D})}(\frac{1}{2} + \lambda_{bf} - \frac{q_0 - q_0^n}{q_0^{n-1} - q_0^n}\frac{\Delta_{n-2}}{2R_0})] \tag{3}$$

where $F_2 = 6\eta_{bf}^{eff} D(n-1)(l\Delta_{l-1}/\eta_{line,l-1})_{avr,n-1}/h_{bf}^2$.

3.3 Performance parameters

3.3.1 For the present multiscale analysis

The dimensionless total volume flow rate through the tube is (Zhang 2020b):

$$Q_v = \frac{K_1}{2\lambda_{bf}}, \text{ for } K_1 > K_{cr} \tag{4}$$

where $Q_v = q_v\eta/(\tau_{s,b-f}h_{bf}^3)$, $q_v = q_{v,bf} + q_{v,hf}$, $K_1 = POW\eta/(\tau_{s,b-f}^2 h_{bf}^2 \Delta l)$, and the dimensionless critical power loss on the tube with the axial length Δl for starting the interfacial slippage is:

$$K_{cr} = \frac{1}{4\lambda_{bf}^2}\{8\pi\frac{R_e}{R_0}\{\frac{\varepsilon\lambda_{bf}^3}{C_y\left(1+\frac{\Delta x}{D}\right)}[1 + \frac{1}{2\lambda_{bf}} - \frac{\Delta_{n-2}(q_0 - q_0^n)}{h_{bf}(q_0^{n-1} - q_0^n)}] - \frac{F_1\lambda_{bf}^3}{6C_y}\} + \frac{\pi}{4} - \frac{4\pi}{C_y}\{\frac{F_2\lambda_{bf}^2}{6} - \frac{\lambda_{bf}}{1+\frac{\Delta x}{D}}[\frac{1}{2} + \lambda_{bf} - \frac{\Delta_{n-2}(q_0 - q_0^n)}{2R_0(q_0^{n-1} - q_0^n)}]\}\} \tag{5}$$

Here $C_y = \eta_{bf}^{eff}/\eta$.

When $K_1 \le K_{cr}$, no interfacial slippage occurs on any interface, the dimensionless total volume flow rate through the tube is (Zhang 2020b):

$$Q_v = \frac{(\pi K_1)^{\frac{1}{2}}}{4\lambda_{bf}^2}\{8\frac{R_e}{R_0}\frac{\varepsilon\lambda_{bf}^3}{C_y\left(1+\frac{\Delta x}{D}\right)}[1 + \frac{1}{2\lambda_{bf}} - \frac{\Delta_{n-2}(q_0 - q_0^n)}{h_{bf}(q_0^{n-1} - q_0^n)}] - \frac{4R_eF_1\lambda_{bf}^3}{3R_0C_y}\} + \frac{1}{4} - \frac{4}{C_y}\{\frac{F_2\lambda_{bf}^2}{6} - \frac{\lambda_{bf}}{1+\frac{\Delta x}{D}}[\frac{1}{2} + \lambda_{bf} - \frac{\Delta_{n-2}(q_0 - q_0^n)}{2R_0(q_0^{n-1} - q_0^n)}]\}\}^{1/2} \tag{6}$$

The ratio of the total mass flow rate through the tube calculated from the present analysis to that calculated from the classical hydrodynamic flow theory (without consideration of any interfacial slippage and any adsorbed layer) is defined as:

$$r_q = \frac{\rho_{bf}^{eff} q_{v,bf} + \rho q_{v,hf}}{q_{m,conv}} \tag{7}$$

where ρ_{bf}^{eff} is the average density of the adsorbed layer across the layer thickness, ρ is the fluid bulk density, and $q_{m,conv}$ is the classical calculation of the mass flow rate through the tube.

The ratio of the mass flow rate of the adsorbed layer to that of the intermediate continuum fluid is defined as: $r_{b/h} = \rho_{bf}^{eff} q_{v,bf}/(\rho q_{v,hf})$.

3.3.2 Based on the solid layer assumption

If the adsorbed layer is taken as a solid layer and the adsorbed layer-fluid interfacial slippage is considered, for the interfacial slippage case, the dimensionless total volume flow rate through the tube is:

$$Q_{v,s} = \frac{K_1}{2\lambda_{bf}}, \text{ for } K_1 > K_{cr,s} \tag{8}$$

where $K_{cr,s}$is the dimensionless critical power loss on the tube with the axial length Δl for starting the interfacial slippage and $K_{cr,s} = \pi/(16\lambda_{bf}^2)$.

When no interfacial slippage occurs on the adsorbed layer-fluid interface, the dimensionless total volume flow rate through the tube is:

$$Q_{v,s} = \frac{\sqrt{\pi K_1}}{8\lambda_{bf}^2}, \text{ for } K_1 \le K_{cr,s} \tag{9}$$

In the case of the interfacial slippage, the ratio of the mass flow rate through the tube calculated based on the solid layer assumption to that calculated from the classical hydrodynamic flow theory is:

$$r_{q,s} = \frac{\frac{4A}{\pi}+1}{(1+2\lambda_{bf})^4}, \text{ for } A \geq 0 \tag{10}$$

where $A = \Delta POW\eta/(\tau_{s,b-f}^2 R_0^2 \Delta l)$.

4. Calculation

It was chosen that $\Delta x/D = \Delta_{n-2}/D = 0.15$. It was equivalently taken that $\eta_{line,i}/\eta_{line,i+1} = q_0^m$, where q_0 and m are respectively positive constants.

It was formulated that (Zhang 2014):

$$Cy(H_{bf}) = a_0 + \frac{a_1}{H_{bf}} + \frac{a_2}{H_{bf}^2} \tag{11}$$

where $H_{bf} = h_{bf}/h_{cr,bf}$, $h_{cr,bf}$ is a critical thickness, and a_0, a_1 and a_2 are respectively constant.

It was formulated that (Zhang 2014):

$$\frac{\rho_{bf}^{eff}}{\rho} = Cq(H_{bf}) = m_0 + m_1 H_{bf} + m_2 H_{bf}^2 + m_3 H_{bf}^3 \tag{12}$$

where τ_s, τ_s, τ_s and τ_s are respectively constants.

The parameters ε, F_1 and F_2 have been respectively regressed out to be (Zhang 2020b):

$$\varepsilon = 4.56\times10^{-6}\left(\frac{\Delta_{n-2}}{D}+31.419\right)(n+133.8)(q_0+0.188)(m+41.62) \tag{13}$$

$$F_1 = 0.18(\Delta_{n-2}/D - 1.905)(\ln n - 7.897) \tag{14}$$

and

$$F_2 = -3.707\times10^{-4}\left(\frac{\Delta_{n-2}}{D}-1.99\right)(n+64)(q_0+0.19)(m+42.43) \tag{15}$$

The weak, medium and strong fluid-tube wall interactions are respectively considered and they have the following parameter values:

Weak interaction: m = 0.5, n = 3, $q_0 = 1.03$, $h_{cr,bf}$ = 7 nm

Medium interaction: m = 1.0, n = 5, $q_0 = 1.1$, $h_{cr,bf}$ = 20 nm

Strong interaction: m = 1.5, n = 8, $q_0 = 1.2$, $h_{cr,bf}$ = 40 nm

The other parameter values are shown in Table 1 (a) and (b).

5. Result

Fig. 2(a) shows the values of r_q and $r_{q,s}$ for different λ_{bf} and A when the fluid-tube wall interaction is weak. For the low values of A such as $A \leq 1$, the value of $r_{q,s}$ is significantly lower than that of r_q when $\lambda_{bf} \geq 0.05$. It means that for these cases the calculation based on the solid layer assumption significantly underestimates the mass flow rate through the tube and the calculation should be based on the multiscale scheme by considering the flowing property of the adsorbed layer. However, for the value of A as high as over 10, the values of r_q and $r_{q,s}$ are very close to one another. This means that for such cases the adsorbed layer can be treated as a solid layer even when the fluid-tube wall interaction is weak. It is due to the effect of the great interfacial slippage, which results in the negligible flowing of the adsorbed layer. Increasing the value of A i.e., increasing the interfacial slippage is shown very effectively to increase the mass flow rate through the tube (i.e., the value of r_q). For large interfacial slippage such as A = 100, the calculated mass flow rate through the tube is two orders higher than the classical hydrodynamic flow theory calculation (i.e., $r_q \approx 100$). These results match the molecular dynamics simulation outcomes (Mattia and Calabro 2012, Myers 2011) for hydrophobic tube walls, which were ascribed to the interfacial slippage effect.

Table 1(a) Fluid viscosity data for different fluid-tube wall interactions (Zhang 2014)

Parameter Interaction	a_0	a_1	a_2
Strong	1.8335	-1.4252	0.5917
Medium	1.0822	-0.1758	0.0936
Weak	0.9507	0.0492	1.6447×10^{-4}

Table 1(b) Fluid density data for different fluid-tube wall interactions (Zhang 2014)

Parameter Interaction	m_0	m_1	m_2
Strong	1.43	-1.723	2.641
Medium	1.30	-1.065	1.336
Weak	1.116	-0.328	0.253

Fig. 2(b) shows the values of r_q and $r_{q,s}$ for the medium fluid-tube wall interaction. For a given A, the curves for r_q and $r_{q,s}$ are much closer than those in Fig. 2(a). It means that for the medium fluid-tube wall interaction the flowing ability of the adsorbed layer is significantly reduced than for the weak fluid-tube wall interaction. The combined effect of the fluid-tube wall interaction and the adsorbed layer-fluid interfacial slippage makes the adsorbed layer able to be treated as a solid layer at a much lower value of A for the medium fluid-tube wall interaction than for the weak fluid-tube wall interaction. Fig. 2(c) shows that for the strong fluid-tube wall interaction the adsorbed layer can be treated as a solid layer when the interfacial slippage occurs (A > 0), as the curves for r_q and $r_{q,s}$ are overlaid for a given A. For this case, the flow ability of the adsorbed layer is lost. It is shown that for the strong fluid-tube wall interaction, if no interfacial slippage occurs, the mass flow rate through the tube is much smaller than the classical theory calculation (as $r_q < 1$ for A=0), However, when the interfacial slippage is large enough (e.g., $A \geq 10$), the mass flow rate through the tube

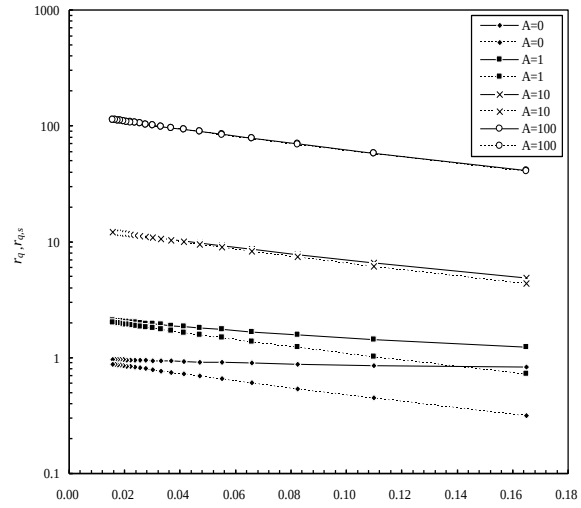

(a) For the weak fluid-tube wall interaction

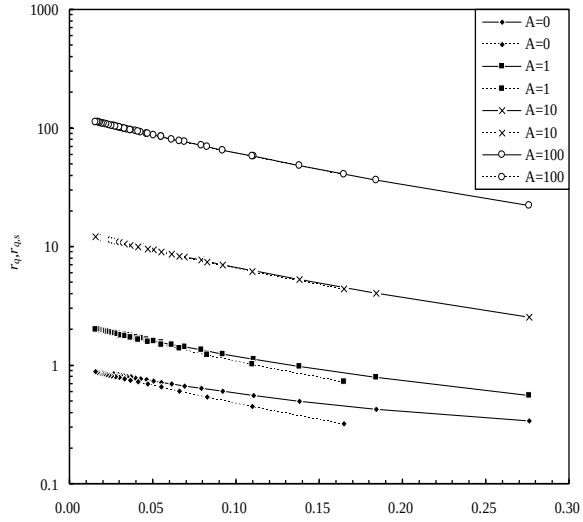

(b) For the medium fluid-tube wall interaction

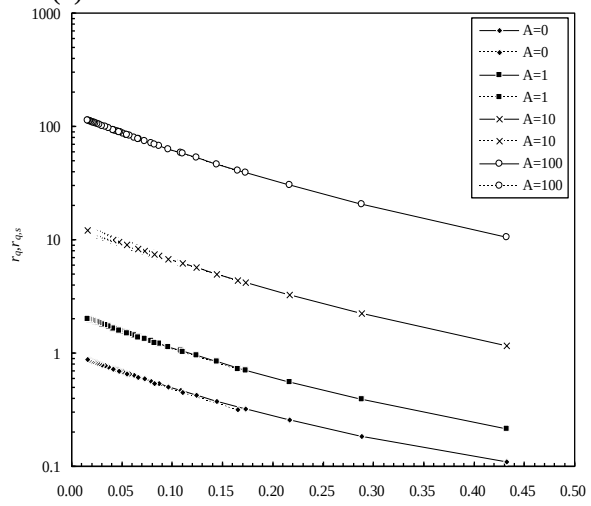

(c) For the strong fluid-tube wall interaction

Fig. 2 Values of r_q and $r_{q,s}$ Solid line for r_q and dashed line for $r_{q,s}$

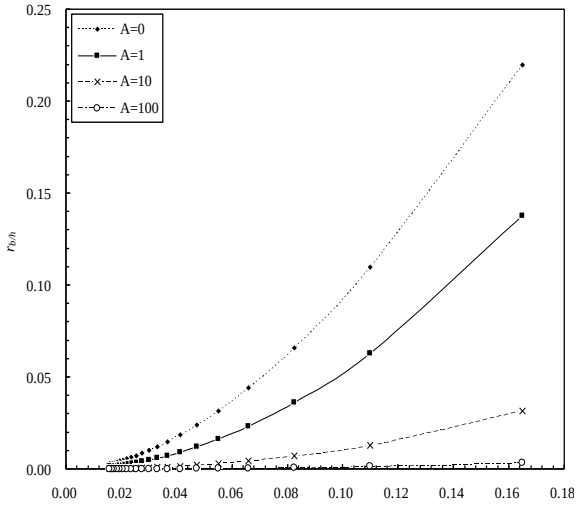

(a) For the weak fluid-tube wall interaction

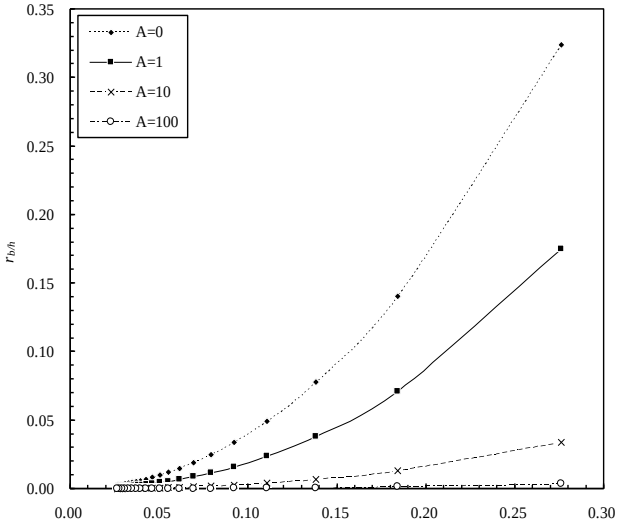

(b) For the medium fluid-tube wall interaction

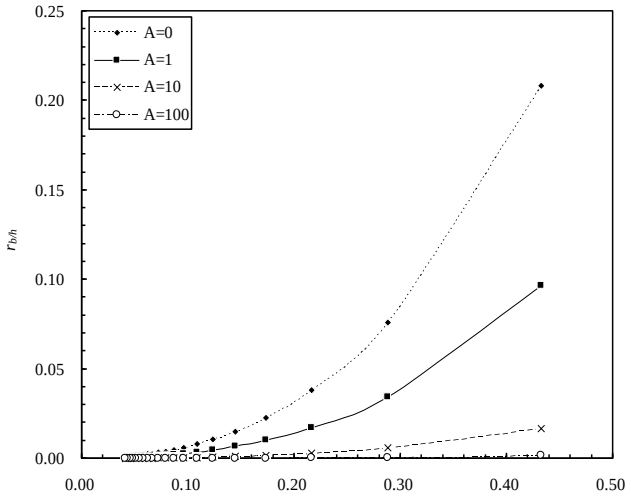

(c) For the strong fluid-tube wall interaction

Fig. 3 Values of $r_{b/h}$.

is still much higher than the classical theory calculation ($r_q > 1$). This shows the great benefit of the interfacial slippage in improving the mass transfer in micro/nano tubes particularly for the strong fluid-tube wall interaction.

Figs. 3(a)-3(c) show the values of $r_{b/h}$ respectively for the weak, medium and strong fluid-tube wall interactions. Whichever the fluid-tube wall interaction is, when the value

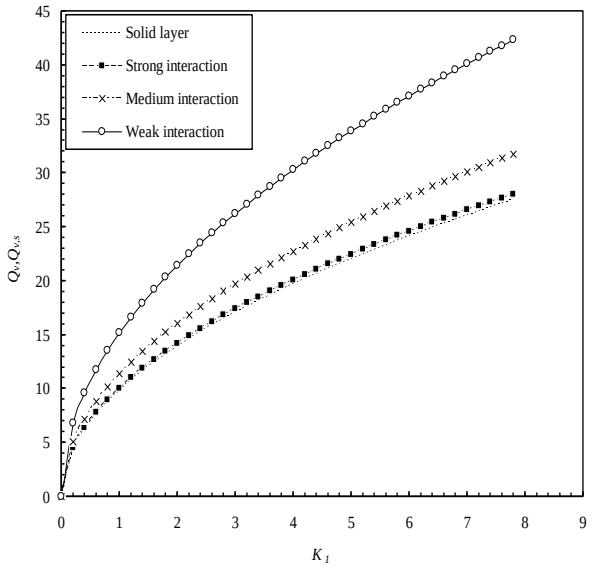

Fig. 4 Values of the dimensionless volume flow rates (Q_v and $Q_{v,s}$) through the tube respectively calculated from the present scheme and the solid layer assumption when λ_{bf} = 0.15

of A is large such as over 100 i.e., the interfacial slippage is large, the value of $r_{b/h}$ is shown to be very low and this indicates the negligible mass flow rate of the adsorbed layer, in this condition, because of the adsorbed layer-fluid interfacial slippage, the intermediate continuum fluid flow almost contributes all of the transported mass, while the adsorbed layer very slowly flows and it can be considered as a solid layer. With the increase of λ_{bf}, the value of $r_{b/h}$ is significantly increased especially for a smaller value of A i.e., a weaker interfacial slippage. Fig. 3(c) shows that even for the strong fluid-tube wall interaction, when A is small such as lower than 1.0, the value of $r_{b/h}$ can be over 0.1 for $\lambda_{bf} > 0.45$. This indicates that the mass transport of the adsorbed layer is normally not negligible when the interfacial slippage is weak and the tube inner diameter is less than four times of the thickness of the adsorbed layer, in spite of the fluid-tube wall interaction.

Fig. 4 compares the values of Q_v calculated respectively for the weak, medium and strong fluid-tube wall interactions when $\lambda_{bf} = 0.15$. These Q_v values are also compared with the value of $Q_{v,s}$ for the same condition. For a given dimensionless power loss K_1, the increase of the fluid-tube wall interaction strength significantly reduces the flow rate through the tube. When the fluid-tube wall interaction is strong, the value of Q_v is very close to that of $Q_{v,s}$. This again indicates that for a strong fluid-tube wall interaction, the adsorbed layer can be taken as a solid layer whenever the interfacial slippage occurs or not, if λ_{bf} is not too large e.g., $\lambda_{bf} \leq 0.15$.

6. Conclusions

The multiscale calculation results are presented for the flow in micro/nano cylindrical tubes when the adsorbed layer-fluid interfacial slippage is considered. The thickness of the adsorbed layer on the tube wall is comparable to the tube inner diameter. The weak, medium and strong fluid-tube wall interactions are respectively considered. The adsorbed layer is treated as in the non-continuum flow which is simulated by the flow factor approach model. The flow within the intermediate continuum fluid is simulated by the Newtonian fluid model.

The calculation results show that when the interfacial slippage is large ($A \geq 10$), the adsorbed layer can be taken as a solid layer in spite of the fluid-tube wall interaction, for large interfacial slippage such as A = 100, the calculated mass flow rate through the tube is two orders higher than the classical Hagen-Poiseuille equation calculation. The interfacial slippage substantially improves the mass transport through the tube. The fluid-tube wall interaction has a great influence on the mass transport through the tube, the increase of the fluid-tube wall interaction strength significantly reduces the flow rate through the tube.

In the calculation, whether the adsorbed layer can be treated as a solid layer depends on the fluid-tube wall interaction and the value of the dimensionless power loss A for motivating the interfacial slippage. Weaker the fluid-tube wall interaction, higher the critical value of A for the adsorbed layer able to be treated as a solid layer. The mass transport of the adsorbed layer is normally not negligible when the interfacial slippage is weak and the tube inner diameter is less than four times of the thickness of the adsorbed layer, in spite of the fluid-tube wall interaction.

The obtained results are of significant interest to the design and application of micro/nano porous filtration membranes where the diameter of the filtration pore is comparable to the thickness of the adsorbed boundary layer so that the multiscale flow occurs.

Conflict of Interest

The authors declare that there is no conflict of interest with this research.

References

Abraham, F.F. (1978), "The interfacial density profile of a Lennard-Jones fluid in contact with a (100) Lennard-Jones wall and its relationship to idealized fluid/wall systems: A Monte Carlo simulation", *J. Chem. Phys.*, **68**(8), 3713-3716. https://doi.org/10.1063/1.436229.

Atkas, O. and Aluru, N.R. (2002), "A combined continuum/DSMC technique for multiscale analysis of microfluidic filters", *J. Comput. Phys.*, **178**(2), 342-372. https://doi.org/10.1006/jcph.2002.7030.

Baker, L.A. and Bird, S.P. (2008), "Nanopores: A makeover for membranes", *Nat. Nanotechnol.*, **3**, 73-74. http://doi.org 10.1038/nnano.2008.13.

Brown, C.E., Everett, D.H., Powell, A.V. and Thome, P.E. (1975), "Adsorption and structuring phenomena at the solid/liquid interface", *Faraday Discuss.*, **59**, 97-108. https://doi.org/10.1039/DC9755900097.

Calabrò, F. (2017), "Modeling the effects of material chemistry on water flow enhancement in nanotube membranes", *MRS Bull.*, **42**(4), 289-293. https://doi.org/0.1557/mrs.2017.58.

Calabrò, F., Lee, K.P. and Mattia, D. (2013), "Modeling flow enhancement in nanochannels: Viscosity and slippage", *Appl. Math. Lett.*, **26**(10), 991-994. https://doi.org/10.1016/j.aml.2013.05.004.

Chan, D.Y.C. and Horn, R.G. (1985), "The drainage of thin liquid films between solid surfaces", *J. Chem. Phys.*, **83**(10), 5311-5324. https://doi.org/10.1063/1.449693.

Chauveteau, G., Tirrell, M. and Omari, A. (1984), "Concentration dependence of the effective viscosity of polymer solutions in small pores with repulsive or attractive walls", *J. Colloid. Interf. Sci.*, **100**(1), 41-54. https://doi.org/10.1016/0021-9797(84)90410-7.

Debye, P. and Cleland, R.L. (1959), "Flow of liquid hydrocarbons in porous vycor", *J. Appl. Phys.*, **30**(6), 843-849. https://doi.org/10.1063/1.1735251.

Derjaguin, B.V., Popovskij, Y.M. and Altoiz, B.A. (1983), "Liquid-crystalline state of the wall-adjacent layers of some polar liquids", *J. Colloid. Interf. Sci.*, **96**(2), 492-503. https://doi.org/10.1016/0021-9797(83)90051-6.

Everett, D.H. and Findenegg, G.H. (1969), "Calorimetric evidence for the structure of films adsorbed at the solid/liquid interface: The heats of wetting of 'Graphon' by some n-alkanes", *Nature*, **223**(5201), 52. https://doi.org/10.1038/223052a0.

Findenegg, G.H. (1971), "The volumetric behavior of hydrocarbon liquids near the graphon surface", *J. Colloid. Interf. Sci.*, **35**(2), 249-253. https://doi.org/10.1016/0021-9797(71)90117-2.

Fissel, W.H., Dubnisheva, A., Eldridge, A.N., Fleischman, A.J., Zydney, A.L. and Roy, S. (2009), "High-performance silicon nanopore hemofiltration membranes", *J. Membr. Sci.*, **326**(1), 58-63. http://doi.org/10.1016/j.memsci.2008.09.039.

Grosse-Rhode, M. and Findenegg, G.H. (1978), "Formation of ordered monolayers of n-alkanes at the cleavage face of nickel chloride", *J. Colloid. Interf. Sci.*, **64**(2), 374-376. https://doi.org/10.1016/0021-9797(78)90375-2.

Jackson, E.A. and Hillmyer, M.A. (2010), "Nanoporous membranes derived from block copolymers: From drug delivery to water filtration", *ACS Nano.*, **4**(7), 3548-3553. http://doi.org/10.1021/nn1014006.

Jung, J., Shin, B., Park, K.Y., Won, S. and Cho, J. (2019), "Pilot scale membrane separation of plating wastewater by nanofiltration and reverse osmosis", *Membr. Water Treat.*, **10**(3), 239-244. https://doi.org/10.12989/mwt.2019.10.3.239.

Kern, H., Rybinski, W.V. and Findenegg, G.H. (1977), "Prefreezing of liquid n-alkanes near graphite surfaces", *J. Colloid. Interf. Sci.*, **59**(2), 301-307. https://doi.org/10.1016/0021-9797(77)90012-1.

Li, N., Yu, S., Harrell, C. and Martin, C.R. (2004), "Conical nanopore membranes: Preparation and transport properties", *Anal. Chem.*, **76**(7) 2025-30. http://dx.doi.org/10.1021/ac035402e.

Liu, J., Chen, S., Nie, X. and Robbins, M.O. (2007), "A continuum-atomistic simulation of heat transfer in micro- and nano- flows", *J. Comput. Phys.*, **227**(1), 279-291. https://doi.org/10.1016/j.jcp.2007.07.014.

Majumder, M., Chopra, N., Andrews, R. and Hinds, B.J. (2005), "Enhanced flow in carbon nanotubes", *Nature*, **438**(7064), 44. https://doi.org/10.1038/438044a.

Mattia, D. and Calabro, F. (2012), "Explaining high flow rate of water in carbon nanotubes via solid-liquid molecular interactions", *Microfluid. Nanofluid.*, **13**(1), 125-130. https://doi.org/10.1007/s10404-012-0949-z.

Mattia, D., Lee, K.P. and Calabrò, F. (2014), "Water permeation in carbon nanotube membranes", *Current Opinion Chem. Eng.*, **4**, 32-37. https://doi.org/10.1016/j.coche.2014.01.006.

Myers, T.G. (2011), "Why are slip lengths so large in carbon nanotubes", *Microfluid. Nanofluid.*, **10**(5), 1141-1145. https://doi.org/10.1007/s10404-010-0752-7.

Nie, X.B., Chen, S. and Robbins, M.O. (2004), "A continuum and molecular dynamics hybrid method for micro- and nano-fluid flow", *J. Fluid Mech.*, **500**, 55-64. https://doi.org/10.1017/S0022112003007225.

Omidvar, M., Soltaneih, M., Mousavi, S.M., Saljoughi, E., Moarefian, A. and Saffaran, H. (2015), "Preparation of hydrophilic nanofiltration membranes for removal of pharmaceuticals from water", *J. Environ. Health.*, **13**(1), 42. https://doi.org/10.1186/s40201-015-0201-3.

Rashidi, H., Meriam, N., Sulaiman, N., Hashim, N.A., Bradford, L., Asgharnejad, H. and Larijani, M. (2020), "Development of the ultra/nano filtration system for textile industry wastewater treatment", *Membr. Water Treat.*, **11**(5), 333-344. https://doi.org/10.12989/mwt.2020.11.5.333.

Sofos, F., Karakasidis, T. and Sarris, I.E. (2020), "Molecular dynamics simulations of ion drift in nanochannel water flow", *Nanomaterials*, **10**(12), 2373. https://doi.org/10.3390/nano10122373.

Sofos, F., Karakasidis, T. and Spetsiotis, D. (2020), "Molecular dynamics simulations of ion separation in nano-channel water flows using an electric field", *Mol. Simulat.*, **45**(17), 1395-1402. https://doi.org/10.1080/08927022.2019.1637520.

Somers, S.A. and Davis, H.T. (1992), "Microscopic dynamics of fluids confined between smooth and atomically structured solid surfaces", *J. Chem. Phys.*, **96**(7), 5389-5407. https://doi.org/10.1063/1.462724.

Sun, J., He, Y. and Tao, W.Q. (2010), "Scale effect on flow and thermal boundaries in micro-/nano- channel flow using molecular dynamics-continuum hybrid simulation method", *Int. J. Numer. Meth. Eng.*, **81**(2), 207-228. https://doi.org/10.1002/nme.2683.

Surwade, S.P., Smirnov, S.N., Vlassiouk, I.V., Unocic, R.R., Veith, G.M., Dai, S. and Mahurin, S.M. (2015), "Water desalination using nanoporous single-layer grapheme", *Nat. Nanotechnol.*, **10**(5), 459-464. https://doi.org/10.1038/nnano.2015.37.

Tiraferri, A., Yip, N.Y., Phillip, W.A., Schiffman, J.D. and Elimelech, M. (2011), "Relating performance of thin-film composite forward osmosis membranes to support layer formation and structure", *J. Membr. Sci.*, **367**(1-2), 340-352. http://doi.org/10.1016/j.memsci.2010.11.014.

Whitby, M. and Quirke, N. (2007), "Fluid flow in carbon nanotubes and nanopipes", *Nat. Nanotechnol.*, **2**(2), 87-94. https://doi.org/10.1038/nnano.2006.175.

Yang, S.Y., Ryu, I., Kim, H.Y., Kim, J.K., Jang, S.K. and Russell, T.P. (2006), "Nanoporous membranes with ultrahigh selectivity and flux for the filtration of viruses", *Adv. Mater.*, **18**(6), 709-712. https://doi.org/10.1002/adma.200501500.

Yen, T.H., Soong, C.Y. and Tzeng, P.Y. (2007), "Hybrid molecular dynamics-continuum simulation for nano/mesoscale channel flows", *Microfluid. Nanofluid.*, **3**(6), 665-675. https://doi.org/10.1007/s10404-007-0202-3.

Yip, N.Y., Tiraferri, A., Phillip, W.A., Schiffman, J.D. and Elimelech, M. (2010), "High performance thin-film composite forward osmosis membrane", *Environ. Sci. Technol.*, **44**(10), 3812-3818. http://doi.org/0.1021/es1002555.

Zhang, Y.B. (2006), "Flow factor of non-continuum fluids in one-dimensional contact", *Industr. Lubr. Tribol.*, **58**(3), 151-169. https://doi.org/10.1108/00368790610661999.

Zhang, Y.B. (2014), "Lubrication analysis for a line contact covering from boundary lubrication to hydrodynamic lubrication: Part I- Micro contact results", *J. Comput. Theor. Nanosci.*, **11**(1), 62-70. https://doi.org/10.1166/jctn.2014.3318.

Zhang, Y.B. (2019), "Power loss in multiscale mass transfer",

Front. Heat Mass Transf., **13**, 22. http://doi.org/10.5098/hmt.13.22.

Zhang, Y.B. (2020a), "Modeling of flow in a very small surface separation", *Appl. Math. Model.*, **82**, 573-586. http://doi.org/10.1016/j.apm.2020.01.069.

Zhang, Y.B. (2020b), "Modeling of flow in a micro cylindrical tube with the adsorbed layer effect: Part II-Results for interfacial slippage", *Int. J. Heat Mass Tran.*, Under Review.

ED